Onset and evolution of the tilted smectic antiphase in a polar liquid-crystal binary mixture

Yushan Shi,[1] George Nounesis,[2] and Satyendra Kumar[1]
[1]*Department of Physics and Liquid Crystal Institute, Kent State University, Kent, Ohio 44242*
[2]*Institute of Radioisotopes and Radiodiagnostic Products, NCSR ''Demokritos'' 153 10 Aghia Paraskevi, Greece*
(Received 27 November 1995)

High-resolution x-ray diffraction studies of a binary mixture of the $n=8$ and $n=10$ homologs of alkoxyphenyl nitrobenzoyloxy benzoate DB_nONO_2 (52.6 mole % $DB_{10}ONO_2$) have been performed at the onset of the tilted smectic antiphase (Sm-$\tilde{C}$) upon cooling from the smectic-A_1 phase. Fluctuations of the two competing smectic orders are found to be related to monolayer and partial bilayer ordering. With decreasing temperature, the period of the antiphase in-plane modulation increases while the smectic layer normal tilts at an angle of $\pm 7°$ with respect to the director. This tilt partially recovers upon the transition to the smectic-A_2 phase. [S1063-651X(96)01108-7]

PACS number(s): 61.30.−v, 68.55.Jk, 78.20.Ci

The classical picture of the smectic-*A* (Sm-*A*) liquid-crystal phase is that of a stack of two-dimensional liquid layers of rodlike molecules. The order can be described by a one-dimensional mass density modulation in the direction of the layer normal. This picture is dramatically altered by the introduction of longitudinal molecular dipoles. The formation of antiferroelectric pairs becomes energetically favorable and this can induce a one-dimensional polarization modulation. Three distinct polymorphic smectic-*A* phases can thus be formed, namely, the monolayer Sm-A_1, the bilayer Sm-A_2, and the partial bilayer Sm-A_d. Although all three possess the same symmetry, they differ in the relative amplitudes and periods of the two modulations. For the Sm-A_1 phase, the smectic periodicity $d=L$ (the molecular length), for Sm-A_2, $d=2L$ and for Sm-A_d, $d=L'$ where $L<L'<2L$.

A remarkable property of several polar smectic systems is the repeated symmetry breaking and recovery (as a function of temperature or composition), due to the appearance of reentrant nematic phases N_r, the smectic antiphase Sm-$\tilde{A}$, or the tilted smectic antiphase Sm-$\tilde{C}$, as intermediate yet thermodynamically stable states between the polymorphic smectic-*A* phases. A phenomenological mean-field theory [1] based on the competition between two fundamental incommensurate length scales, i.e., the molecular length L and the antiferroelectric dimer length L', has been very successful in describing the polymorphism of polar smectics. The nematic reentrance phenomena has been explained as a means of escaping antiferroelectric frustration by the onset of positional disorder. The occurrence of smectic antiphases [Sm-$\tilde{A}$ and Sm-$\tilde{C}$] is a consequence of the development of an in-plane density modulation, to escape imminent incommensurability.

The reentrances of the nematic phase in frustrated smectic systems have been studied extensively and fluctuations of competing periodicities have been found to play a very important role [2]. Fluctuations are also responsible for exotic behavior within the reentrant range such as the theoretically predicted phase transition between two uniaxial nematics characterized by strong monolayer and bilayer correlations. This transition was recently observed [3] experimentally. While the transition from Sm-A_1 to the antiphase Sm-$\tilde{A}$ has been studied in detail [4], the onset of the Sm-$\tilde{C}$ phase has not. In this paper we present a high-resolution x-ray diffraction study of the Sm-A_1–Sm-$\tilde{C}$ phase transition. We find that the competition between the two incommensurate [monolayer and partial bilayer] smectic order fluctuations plays an important role at this weakly first order transition. Our results on the binary mixture of the $n=8$ and $n=10$ homologs of DB_nONO_2 (52.6 mole % $DB_{10}ONO_2$) demonstrate that the diffraction peaks at the Sm-A_1–Sm-$\tilde{C}$ phase transition condense into two pairs of off-axis quasi-Bragg peaks in the Sm-$\tilde{C}$ phase. The period of the antiphase modulation increases gradually as the incommensurability between the two density waves decreases and discontinuously becomes infinite at the transition to the Sm-A_2 phase. The normal to different sections of smectic layers in the antiphase is tilted alternatingly at 7° in opposite directions with respect to the director defined by an external magnetic field.

The experiment was conducted using a four-circle x-ray diffractometer with an 18 k W Cu rotating anode source and a pair of Ge(111) single crystals as monochromator and analyzer that gave a longitudinal resolution $\Delta Q_\parallel = 4\times10^{-4}$ Å^{-1}. The out-of-plane transverse resolution is $\Delta Q_z = 10^{-2}$ Å^{-1}. Experimental details have been described elsewhere [5]. A Siemens X1000 diffractometer equipped with an area detector was used to obtain global features of the diffraction patterns. Approximately 100 mg of the sample was sealed between two 10 μm thick mylar sheets and placed in an oven with a temperature stability of ± 0.01 K. The sample was initially aligned in the nematic phase ($T>200$ °C) and then cycled through the Sm-A_d phase and the reentrant nematic phase several times in the presence of *in situ* (6.5 kG) magnetic field produced by a pair of permanent magnets, to ensure good alignment. The two fundamental lengths, L' and L, were determined from the peak positions of the quasi-Bragg peaks, $\mathbf{q}'$ in the Sm-A_d phase and $2\mathbf{q}_0$ in the Sm-A_1 phase in the proximity of the reentrant N phase, and found to be 46.0 Å and 30.8 Å, respectively.

We measured the evolution of the reflections at $2\mathbf{q}_0$ and $\mathbf{q}'$ as the Sm-$\tilde{C}$ phase was approached on cooling. The evolution of the density wave with wave vector $2\mathbf{q}_0$ at the Sm-A_1–Sm-$\tilde{C}$ transition is shown in Fig. 1. The ten iso-intensity

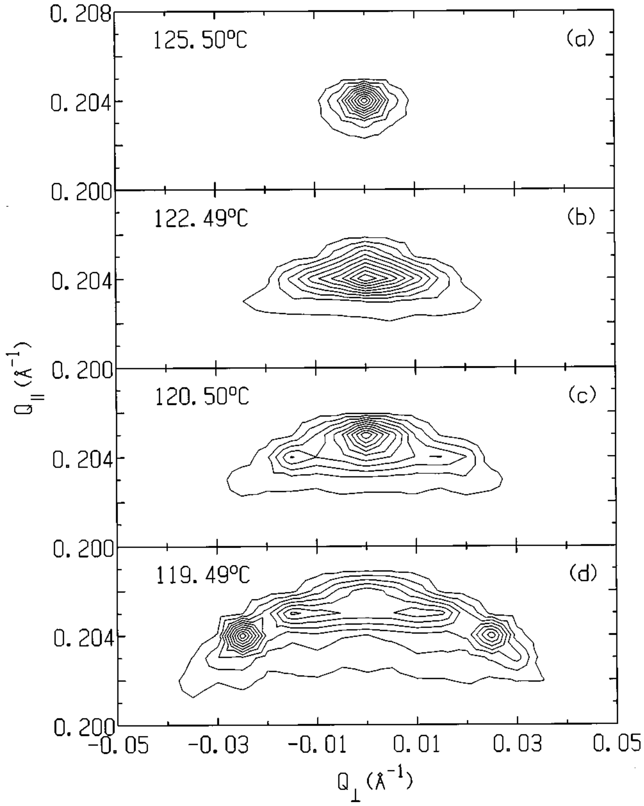

FIG. 1. Evolution of the $2\mathbf{q}_0$ peak at the Sm-A_1-$\widetilde{C}$ phase transition. (a) The $2\mathbf{q}_0$ peak is resolution limited in the A_1 phase. (b, c) It gradually broadened and moved to higher values of scattering vectors giving a decrease of 0.7% in smectic layer spacing in 5 K with decreasing temperature. (d) The tilted layer segments with ± 7 degree layer tilt developed at this transition as evidenced by the growth of two off-axis peaks.

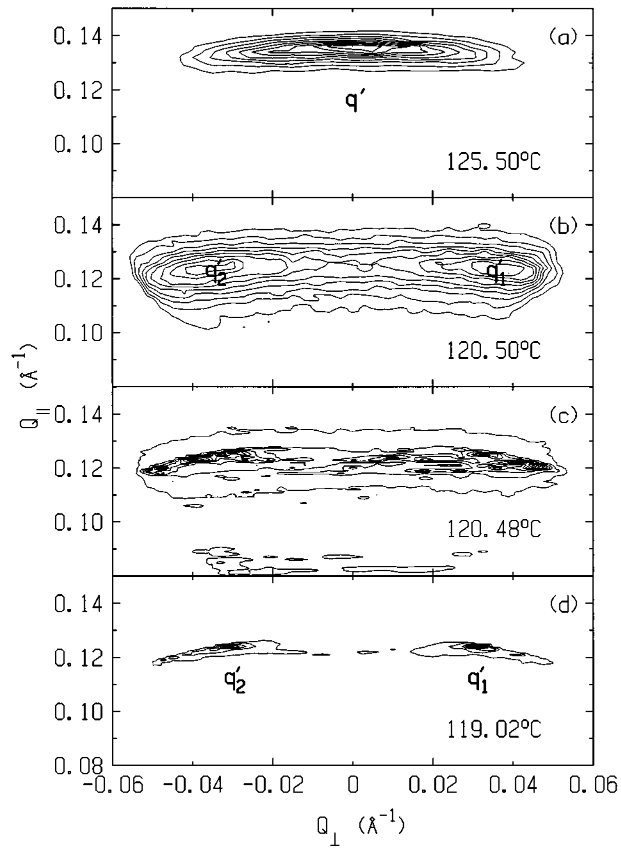

FIG. 2. Onset and temperature dependence of antiphase modulation indicated by changes in scattering at $\mathbf{q}'=0.1350$ Å. (a) In the A_1 phase, the diffuse $\mathbf{q}'$ peak was due to the A_d phase fluctuations. (b) The antiphase fluctuations gradually developed and produced off-axis diffuse scattering at $\mathbf{q}_1'$ and $\mathbf{q}_2'$. (c) Diffuse scattering due to broad mosaic arose from layer tilt. (d) The development of the antiphase modulation was indicated by the condensation of the $\mathbf{q}_1'$ and $\mathbf{q}_2'$ peaks. Note that only the $\mathbf{q}_1'$ and $\mathbf{q}_2'$ peaks are visible in the high-resolution results shown here.

contours are evenly spaced between the maximum and background intensities. At approximately 5 K above the transition, at 125.50 °C [Fig. 1(a)], the condensed quasi-Bragg peak was located at (0, 0, 0.2040) Å^{-1} with resolution limited full width at half maximum (FWHM) of 0.0008 Å^{-1} along $Q_{\parallel}$. In the transverse direction, the peak was mosaic limited with 0.0053 Å^{-1} FWHM. The in-plane transverse correlation length was estimated to be at least 380 Å^{-1}. The transverse width, primarily due to layer undulations that develop upon approaching the Sm-$\widetilde{C}$ phase, increased [Figs. 1(b) and 1(c)] at a linear rate of 1.2 °/K with decreasing temperature accompanied by a decrease in the layer spacing at a rate of -0.14%/K. This broadening has been interpreted [6] as evidence that the Sm-A_1–Sm-$\widetilde{C}$ transition is mediated by smectic-C-like fluctuations of the orientational order. At T = 120.50 °C, just 10 mK above the transition temperature ($T_{A_1-\widetilde{C}}=120.49$ °C), the angular peak width and the fractional layer-spacing change ($\Delta L/L$) attained the values of 8° and -0.7%, respectively. At T=120.48 °C, 10 mK below $T_{A_1-\widetilde{C}}$, two off-axis peaks appeared at (± 0.025, 0, 0.2040) Å^{-1}, at $\pm 7°$ with respect to the monolayer peak (i.e., the director, defined by the direction of the magnetic field). The positions of these two peaks did not change as the temperature was lowered, but they gained intensity at the expense of the on-axis Sm-A_1 peak, Fig. 1(d). The widths of the off-axis peaks in $Q_{\parallel}$ and $Q_{\perp}$ directions were comparable to that of the on-axis Sm-A_1 peak ($2\mathbf{q}_0$) at 125.50 °C, Fig. 1(a). The difference in their intensities could be accounted for by the experimental geometry and initial alignment [3]. ω scans of both off-axis peaks were identical [7,8] suggesting that these reflections originated from the same scattering volume. This led us to conclude that the smectic layers attain a zigzag shape at the transition to the antiphase Sm-$\widetilde{C}$ with adjacent layer segments making an angle of 14° with each other which is two times the angle of 7° between the local smectic layer normal and the director.

The evolution of the $\mathbf{q}'$ peak at the onset of the antiphase modulation is shown in Fig. 2. In the Sm-A_1 phase, Fig. 2(a), the diffuse $\mathbf{q}'$ peak at (0, 0, 0.1350) Å^{-1} arose from the Sm-A_d fluctuations [9]. The presence of the antiphase fluctuations are indicated by the two off-axis diffuse peaks at $\mathbf{q}_1'$ and $\mathbf{q}_2'$ which began developing at approximately 124.85 °C, in the Sm-A_1 phase [9]. These peaks gradually moved to a lower value of $Q_{\parallel}$ with increasing intensities as the Sm-A_1–Sm-$\widetilde{C}$ transition was approached, Fig. 2(b).

At the Sm-A_1–Sm-$\widetilde{C}$ transition, two pairs, i.e., $\mathbf{q}_1'$, $\mathbf{q}_1''$ and $\mathbf{q}_2'$, $\mathbf{q}_2''$, appeared (Fig. 3) at the same time as the two reflec-

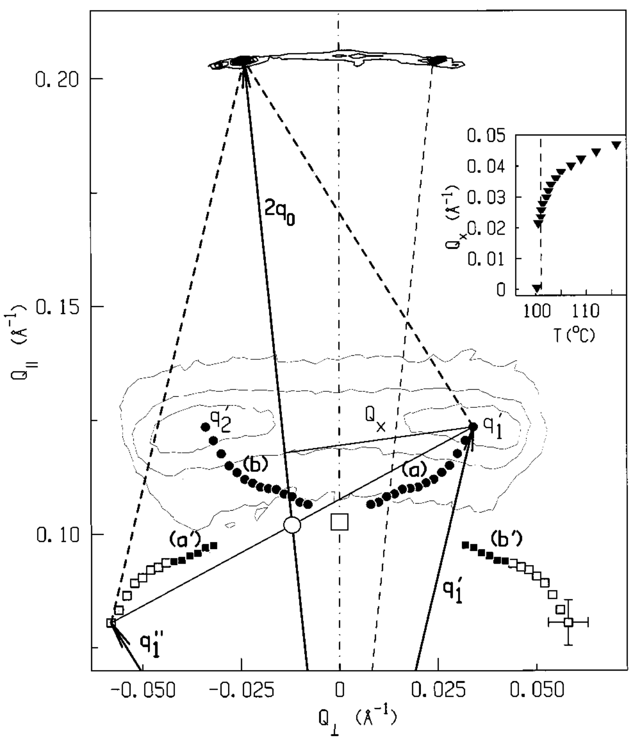

FIG. 3. Temperature dependence of the off-axis $\mathbf{q}_1'$, $\mathbf{q}_2'$, and $(2\mathbf{q}_0-\mathbf{q}_1')$ peaks and the on-axis $(2\mathbf{q}_0)$ peaks in the antiphase Sm-$\tilde{C}$. The $2\mathbf{q}_0$ peak remained stationary. The positions of antiphase peaks indicated by segments a and b were measured at 119.0, 116.0, 112.0, 109.0, 107.0, 105.0, 104.0, 103.0, 102.5, 102.1, 101.4, 101.1, 101.0, and 100.5 °C. The shaded squares on segment a' were obtained from a low resolution experiment. Representative uncertainties in the value of the scattering vector as shown on one point. This peak moved towards $2\mathbf{q}_0/2$ (big open circle). The vectors represent the positions of the scattering peaks in reciprocal space at 119.00 °C. The contour map is a plot of the Sm-$\tilde{C}$ fluctuation measured at 120.5 °C. The dependence on temperature of the in-plane modulation $\mathbf{Q}_x$ is shown in the inset. At the temperature below the transition (dashed line), the two phases Sm-$\tilde{C}$ and Sm-A_2 were found to coexist.

tions at ($\pm$0.025, 0, 0.2040) Å^{-1}. The centers of $\mathbf{q}_1''$ and $\mathbf{q}_2''$ peaks were not accessible in the high-resolution scans due to a limited angular range of the oven. Their positions were later determined with a Siemens diffractometer and a different oven with wider angular access. The sum of the wave vectors of these pairs was exactly equal to the value of the scattering vector of the corresponding higher peak, i.e., $\mathbf{q}_1'+\mathbf{q}_1''=(-0.025,\ 0,\ 0.2040)$ Å^{-1} and $\mathbf{q}_2'+\mathbf{q}_2''=(+0.025,\ 0,\ 0.2040)$ Å^{-1}. The incommensurate, orientational, and antiphase fluctuations became comparable resulting in a broad specklelike pattern shown in Fig. 2(c).

The antiphase was fully developed at 119.02 °C. As shown in Fig. 2(d), the diffuse scattering condensed into two pairs of resolution limited peaks; $\mathbf{q}_1'$, $\mathbf{q}_1''(=2\mathbf{q}_0-\mathbf{q}')$ with $2\mathbf{q}_0=(-0.025,\ 0,\ 0.2040)$ Å^{-1} for one pair and $\mathbf{q}_2'$, $\mathbf{q}_2''$ $(=2\mathbf{q}_0-\mathbf{q}_2')$ with $2\mathbf{q}_0=(+0.025,\ 0,\ 0.2040)$ Å^{-1} for the other. The position of the $\mathbf{q}_1''$ peak is shown by shaded squares on segment a' in Fig. 3. The observed double peaks at ($\pm$ 0.025, 0, 0.2040) were due to the intrinsic structure of

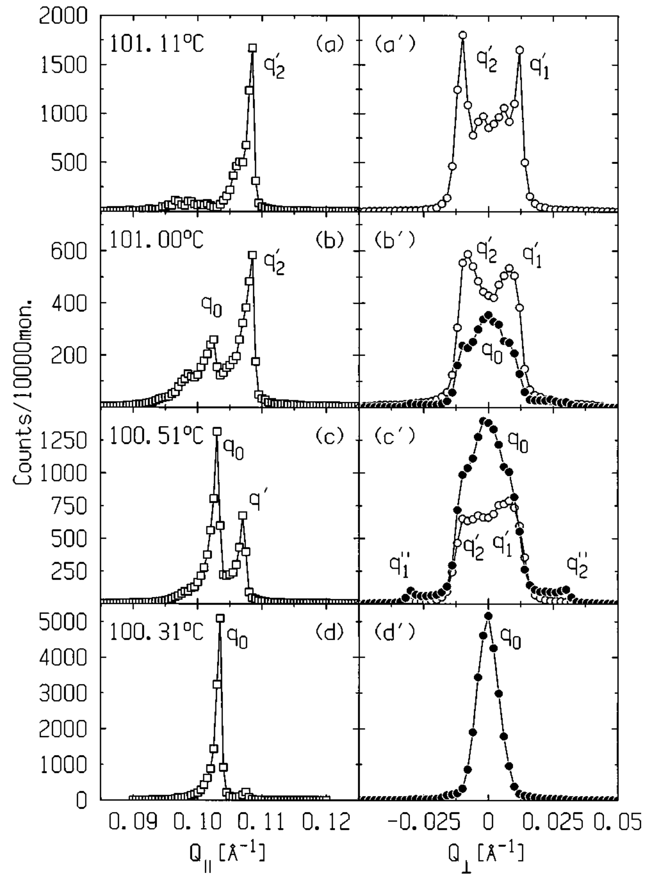

FIG. 4. Longitudinal and transverse scans of $\mathbf{q}_1'$, $\mathbf{q}_2'$, and $\mathbf{q}_0$ scattering at the Sm-$\tilde{C}$-A_2 transition. (a) and (a$'$): double off-axis antiphase peaks. (b) and (b$'$): double off-axis antiphase peaks with a single on-axis condensed peak at $\mathbf{q}_0$. (c) and (c$'$): single condensed peak at $\mathbf{q}_0$ gained intensity while the double antiphase peaks became diffuse with decreasing temperature. (d) and (d$'$): double off-axis antiphase peaks disappeared as the sample entered the Sm-A_2 phase. Vertical axis shows counts per 10 000 monitor counts.

the Sm-$\tilde{C}$ layers which tilt symmetrically in a zigzag manner with respect to the director.

The segments a, a' and b, b' in Fig. 3, depict the locus of the peaks at $\mathbf{q}_1'$, $\mathbf{q}_1''$ and $\mathbf{q}_2'$, $\mathbf{q}_2''$, respectively, with the temperature decreasing from 119.02 to 100.50 °C. The $2\mathbf{q}_0$ scattering profile did not change within the range of the Sm-$\tilde{C}$ phase.

The projection of the incommensurate wave vector q_1' onto the smectic layer normal was $\delta k = q_1' \cos\alpha$. Here, α (= 22.1°) is the angle between $2\mathbf{q}_0 = (-0.025,\ 0,\ 0.2040)$ Å^{-1} and $\mathbf{q}_1'=(0.034,\ 0,\ 0.1235)$ Å^{-1} at 119.02 °C. The period of the antiphase modulation increased from approximately 130 Å at 119.02 °C to 240 Å at 101.40 °C as evidenced by decreasing $\mathbf{Q}_x$ components of $\mathbf{q}_1'$ and $\mathbf{q}_1''$. This monotonic change continued and the two reflections appeared to be approaching the lockin position indicated by the large open circle. However, before they could converge at this point, the weakly first order transition to the A_2 phase took place and they jumped to the on-axis $\mathbf{q}_0$ position, shown as open square. At the same time the on-axis $2\mathbf{q}_0$ peak (at the roughly same position as in the Sm-A_1 phase) became much brighter than the Sm-$\widetilde{C}$ peaks at (± 0.025, 0, 0.2040) $Å^{-1}$. It should be noted that, as shown in Fig. 3, segments b and b' follow a path analogous to that of a and a'.

Figure 4 shows the longitudinal and transverse scans through various peaks at the Sm-$\widetilde{C}$–Sm-A_2 transition. In (a) and (a′), at 101.11 °C, the two antiphase peaks were located at (± 0.012, 0, 0.1085) $Å^{-1}$ and some diffuse scattering was centered at (0, 0, 0.0980) $Å^{-1}$. In scans (b) and (b′) at 101.00 °C, the antiphase peaks moved closer and towards (± 0.010, 0, 0.1083) $Å^{-1}$. At temperatures below 101 °C, a single condensed peak gradually developed at (0, 0, 0.1025) $Å^{-1}$, commensurate with the on-axis $2\mathbf{q}_0$ peak at (0, 0, 0.2050) $Å^{-1}$. The commensurate on-axis peaks gained intensity marking the advent of the bilayer Sm-A_2 phase. In (c) and (c′), at 100.51 °C, the single condensed peak, located now at (0, 0, 0.1030) $Å^{-1}$, coexisted with the double antiphase peaks at (± 0.008, 0, 0.1065) $Å^{-1}$. As shown in (d) and (d′) at 100.31 °C the two antiphase peaks finally disappeared. At the same temperature and after equilibration time of about 10 minutes, the ω scans of the peaks at $2\mathbf{q}_0$ (= 0.2090 $Å^{-1}$) and $\mathbf{q}_0$ (= 0.1045 $Å^{-1}$) peaks were found to be identical. The system eventually crystallized at 87.30 °C.

In summary, we have observed pretransitional effects and studied, in detail, the onset and evolution of the tilted antiphase Sm-$\widetilde{C}$ in a binary mixture of polar liquid crystal. The in-plane antiphase modulation, in this phase, fully developed approximately at 1.5 K below the transition temperature. The period of antiphase modulation increased monotonically as the incommensurability of the two modulations along the smectic layer normal decreased and eventually became infinite at the transition to the Sm-A_2 phase.

The authors thank S. Pfeiffer for synthesizing the compounds, M. Sutton, C.W. Garland, P. Heiney, and A. M. Levelut for helpful discussions, and acknowledge the use of Siemen's X1000 diffractometer at the Liquid Crystal Institute. This research was supported by the NSF Science and Technology Center ALCOM Grant No. DMR-89-20147.

[1] J. Prost and P. Barois, J. Chem. Phys. **80**, 65 (1983). In this paper the antiphase Sm-$\widetilde{A}$ was considered as a special case of the antiphase Sm-$\widetilde{C}$; J. Wang and T. C. Lubensky, J. Phys. (Paris) **45**, 1653 (1983); P. Barois, J. Prost, and T. C. Lubensky, *ibid.* **46**, 391 (1985).
[2] J. Prost and J. Toner, Phys. Rev. A **36**, 5008 (1987).
[3] G. Nounesis, S. Kumar, S. Pfeiffer, R. Shashidhar, and C.W. Garland, Phys. Rev. Lett. **73**, 565 (1994).
[4] C.R. Safinya, W.A. Varady, L.Y. Chiang, and P. Dimon, Phys. Rev. Lett. **57**, 432 (1986).
[5] Y. Shi, G. Nounesis, C. Garland, and S. Kumar (unpublished).
[6] E. Fontes, P.A. Heiney, J.L. Haseltine, and A.B. Smith III, J. Phys. (Paris) **47**, 1533 (1986).
[7] M.J. Young, L. Wu, G. Nounesis, C.W. Garland, and R.J. Birgeneau, Phys. Rev. E **50**, 368 (1994).
[8] J.T. Mang, B. Cull, Y. Shi, P. Patel, and S. Kumar, Phys. Rev. Lett. **74**, 4241 (1995).
[9] C.W. Garland, in *Geometry and Thermodynamics*, edited by J.-C. Toledano (Plenum, New York, 1990), p. 221; the Sm-A_1 phase with double off-axis diffuse peaks was defined as the Sm-A_1' phase in this paper.